

## MODE MODEL FOR INFRARED PROPAGATION IN A TOROIDAL TYPE OF WAVEGUIDE AND APPLICATIONS

Z. Menachem, N. Croitoru<sup>a\*</sup>, J. Aboudi

Department of Solid Mechanics, Materials and Structures, Faculty of Engineering, Tel-Aviv University, Ramat Aviv 69978, Israel

<sup>a</sup>Department of Physical Electronics, Faculty of Engineering, Tel-Aviv University, Israel

An improved approach is derived for the propagation of electromagnetic (EM) fields along a curved dielectric waveguide. The objective is to develop a mode model to provide a numerical tool for the calculation of the output fields also for intermediate radius of curvature ( $R \approx 0.5$  m). Therefore, we take into account all the terms in the calculations, without neglecting the terms of the bending. The longitudinal components of the fields are developed into Fourier-Bessel series. The transverse components of the fields are expressed as functions of the longitudinal components in the Laplace plane and are obtained by using the inverse Laplace transform. The separation of variables is obtained by using the orthogonal relations. The metal boundaries of the waveguides are modeled as a lossy dielectric media. This model is applicable for hollow waveguide tubes where the wall of the bore is covered with a metal layer and dielectric overlayer.

(Received August 18, 2003; accepted August 28, 2003)

*Keywords:* Wave propagation, Dielectric waveguides, Curved waveguides, Power transmission

### 1. Introduction

Dielectric-coated metallic waveguides have attracted considerable applications in practice and theory for a wide variety of transverse profiles. The development of the fibers and waveguides for the transmission of  $CO_2$  laser infrared (IR) radiation ( $\lambda=10.6$   $\mu\text{m}$ ) is very important for the application of this radiation in medical and industrial fields. A review of the papers on fibers for IR transmission was published [1]. To reduce the transmission losses, the use of hollow core waveguides was proposed because the air is a material with very low transmission losses in the IR region of the spectrum. Hollow fibers are leaky waveguides, because the refractive index of the core material (air) is lower than that of the cladding material dielectric coating [2-4]. The transmission medium is air and the guiding is achieved by refracting (dielectric) and reflecting (metal) layers deposited on the inner surface of the waveguide. Hollow waveguides with both metal and dielectric internal layers were proposed to reduce the transmission losses. A hollow waveguide can be made, in principle, from any flexible or rigid tube (plastic, glass, metal, etc.) if its inner hollow surface (the core) is covered by metal layer and dielectric overlayer. This layer structure enables us to transmit both the TE and TM polarization with low attenuation [4,5].

Various methods for the analysis of cylindrical hollow metallic or metallic with inner dielectric coating waveguides have been studied in the literature [2-11]. Two theoretical models can describe the radiation propagation in a hollow guide. One is based on a mode model [2-7] and the other is based on a ray model [8-11].

---

\* Corresponding author: croitoru@eng.tau.ac.il

The first theoretical analysis of the problem of hollow cylindrical bent waveguides was published by Marcatili and Schmeltzer [2]. Their theory considers the bending as a small disturbance and uses cylindrical coordinates to solve Maxwell equations. They derive the mode equations of the disturbed waveguide using the ratio of the inner radius  $r$  on the curvature radius  $R$  as a small parameter ( $r/R \ll 1$ ). Their theory predicted that the bending will have little influence on the attenuation of a hollow metallic waveguide. However, practical experiments have shown a large increase in the attenuation, even for a rather large  $R$ . Miyagi et al.[3] suggested an improved solution, which provided agreement with the experimental results, but only for  $R \gg r$ . A different approach [4,5] treats the bending as a perturbation that couples the modes of a straight waveguide. That theory explains qualitatively the large difference between the metallic and metallic-dielectric bent waveguide attenuation. The reason for this difference is that in metallic waveguides the coupling between the TE and TM modes caused by the bending mixes modes with very low attenuation and modes with very high attenuation, whereas in metallic-dielectric waveguides, both the TE and TM modes have low attenuation. The EH and HE modes have similar properties and can be related to modes that have a large TM component.

Several methods of investigation of propagation were developed using ray models [8-11]. The problem of transmission of  $CO_2$  laser radiation through hollow fibers and waveguides was studied theoretically and confirmed experimentally by Croitoru et al. [9] It was shown theoretically and proved experimentally that the transmission of  $CO_2$  radiation is possible even through a bent waveguide. An improved ray model for simulating the transmission of laser radiation through a metallic or metallic-dielectric multibent hollow cylindrical waveguide was proposed [10].

The models based on the perturbation theory solve problems only for a large radius of curvature ( $R \gg r$ ). The objective of this work was to develop a theoretical mode model to provide a numerical tool for the calculation of the output transverse fields and power density also for intermediate radius of curvature

( $R \approx 0.5$  m). Therefore we take into account all the terms in the calculations without neglecting the terms of the bending (namely, up to the fourth order of  $1/R$ ). These terms of the bending are functions of  $h_\zeta$ ,  $h_\zeta^2$ ,  $h_\zeta^3$ , and  $h_\zeta^4$  ( $h_\zeta = 1 + (r/R)\sin\theta$ ), where  $h_\zeta$  is the metric coefficient. Thus the maximum value of the bending is of the order of  $1/R^4$ . This will enable us to understand more precisely the influence of the bending on the output fields, output power density, and output power transmission of hollow waveguides. This model was applied in the case of hollow flexible tubes, where the wall of the bore was covered with a metal layer and dielectric overlayer (hollow waveguide). The results of this model were applied to the study of hollow waveguide that are suitable for transmitting infrared radiation, especially  $CO_2$  laser radiation.

## 2. The derivation

The toroidal system  $(r, \theta, \zeta)$  in conjunction with the curved waveguide is shown in Fig. 1. The torus transformation of the coordinates is given by

$$X = (R + r \sin \theta) \cos \left( \frac{\zeta}{R} \right), \quad Y = (R + r \sin \theta) \sin \left( \frac{\zeta}{R} \right), \quad Z = r \cos \theta, \quad (1a, b, c)$$

where  $\zeta = R \phi$ . In this toroidal system the metric coefficients are

$h_r = 1$ ,  $h_\theta = r$ ,  $h_\zeta = 1 + (r/R) \sin \theta$  and a differential length is given by

$ds^2 = h_r^2 dr^2 + h_\theta^2 d\theta^2 + h_\zeta^2 d\zeta^2$  where  $R$  is the bending radius, and  $r$  is the cross-section radius of the waveguide. The case for the straight waveguide is obtained by letting  $R \rightarrow \infty$ .

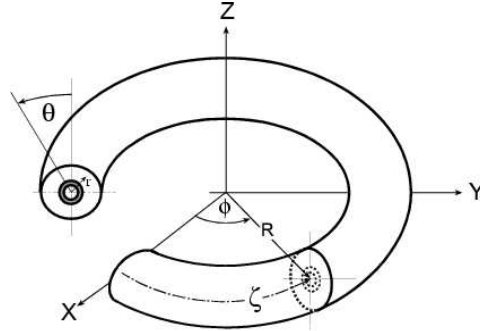


Fig. 1. A general scheme of the toroidal system and the curved waveguide.

The derivation is based on Maxwell's equations for the computation of electromagnetic fields and the radiation power density at each point during propagation through a curved waveguide, in the case of a metallic waveguide (e.g., Ag) with a radial dielectric profile. The longitudinal components of the fields are developed into Fourier-Bessel series. The transverse components of the fields are expressed as a function of the longitudinal components in the Laplace plane.

The modes excited at  $\zeta = 0$  in the waveguide by the conventional  $\text{CO}_2$  laser IR radiation ( $\lambda=10.6 \mu\text{m}$ ) are closer to the  $TEM$  polarization of the laser radiation. The  $TEM_{00}$  mode is the fundamental and the most important mode. This means that a cross section of the beam has a Gaussian intensity distribution. The initial fields at  $\zeta=0^+$  are formulated by using Fresnel coefficients of the transmitted fields as follows

$$E_{r0}^+ = T_E(r)(E_0 e^{-(r/w_0)^2} \sin \theta), \quad E_{\theta 0}^+ = T_E(r)(E_0 e^{-(r/w_0)^2} \cos \theta), \quad (2a, b)$$

$$H_{r0}^+ = -T_H(r)((E_0 / \eta_0) e^{-(r/w_0)^2} \cos \theta), \quad H_{\theta 0}^+ = T_H(r) ((E_0 / \eta_0) e^{-(r/w_0)^2} \sin \theta), \quad (2c, d)$$

where  $E_{\zeta 0}^+ = H_{\zeta 0}^+ = 0$ ,  $T_E(r) = 2/[n(r) + 1]$ ,  $T_H(r) = 2n(r)/[n(r) + 1]$  and  $n(r) = [\epsilon_r(r)]^{1/2}$ . The index of refraction is denoted by  $n(r)$ .

The transverse components of the fields are finally expressed in a form of a *transfer matrix functions* as follows

$$\begin{aligned} E_r(r, \theta, \zeta) = & E_{r0}^+(r) e^{-jk h_\zeta \zeta} - \frac{j \omega \mu_0}{R} h_\zeta \sum_m C_{S1}^m(\zeta) J_1(\psi) \cos^2 \theta \\ & - \frac{j \omega \mu_0}{R} h_\zeta \sin \theta \cos \theta \sum_m D_{S1}^{m'}(\zeta) J_1(\psi) + \frac{j \omega \mu_0}{r} h_\zeta^2 \sin \theta \sum_m C_{S1}^{m'}(\zeta) J_1(\psi) \\ & - \frac{j \omega \mu_0}{r} h_\zeta^2 \cos \theta \sum_m D_{S1}^{m'}(\zeta) J_1(\psi) + \frac{1}{R} \sin \theta \cos \theta \sum_m A_{S2}^{m'}(\zeta) J_1(\xi) \\ & + \frac{1}{R} \sin^2 \theta \sum_m B_{S2}^{m'}(\zeta) J_1(\xi) + h_\zeta \cos \theta \sum_{m'} A_{S2}^{m'}(\zeta) \frac{dJ_1}{dr}(\xi) + h_\zeta \sin \theta \sum_{m'} B_{S2}^{m'}(\zeta) \frac{dJ_1}{dr}(\xi), \quad (3a) \end{aligned}$$

where  $\psi = [P_{1m}^*(r/a)]$ ,  $\xi = [P_{1m}^*(r/a)]$ ,  $m' = 1, \dots, N$ ,  $3 \leq N \leq 50$ .

$A_{S1}^{m'}(\zeta) = L^{-1}[[A_{1m}(s)]/[s^2 + k^2(r)h_\zeta^2]]$ , etc. Similarly, the other transverse components of the fields are obtained.

The inverse Laplace transform is performed in this study by a direct numerical integration in the  $s$ -plane by the residue method. According to the residue method, two dominant poles for the toroidal dielectric waveguide are given by  $s = \pm j k(r)h_\zeta$ , where  $h_\zeta = 1 + (r/R)\sin\theta$ .

The  $\zeta$  component of the average power density Poynting vector is given by  $S_{av} = \frac{1}{2} \text{Re}(E_r H_\theta^* - E_\theta H_r^*)$  where the asterisk indicates the complex conjugate and the total average

power transmitted across a cross section of the guide in the  $\zeta$  direction is given by a double integral of  $S_{av}$ .

### 3. Examples of this mode model

This section presents several examples that demonstrate features of the proposed mode model derived in the previous section. The cross section of the curved waveguide is made of a tube of various types of material, metal layer, and a dielectric layer upon it. The next examples represent the case of hollow waveguide with metallic (Ag) coated by thin dielectric layer (AgI). For silver having a conductivity of  $6.14 \times 10^7 (\text{ohm} \times \text{m})^{-1}$ , and the skin depth at  $10.6 \mu\text{m}$  is  $1.207 \times 10^{-8} \text{ m}$ .

#### Test case

The test case for the straight waveguide is obtained by letting  $R \rightarrow \infty$ . The transmitted fields of the initial fields ( $TEM_{00}$  mode in excitation) are formulated by using Fresnel coefficients [Eqs. (2a) to (2d)]. The results of the output transverse components of the output fields (e.g.,  $|E_r|$ ) and the output power density are shown in Figs. 2(a) and 2(b), respectively. The result of the output power density of this example [Fig. 2(b)] is compared to the results of the previously published experimental data [12] of which the behavior has shown good agreement (a Gaussian shape), as expected, except in the secondary small propagation mode. In this example, the length ( $\zeta(R=\infty)$ ) of the straight waveguide is 1 m, the diameter (2a) of the waveguide is 2 mm, the thickness of the dielectric layer [ $d_{(AgI)}$ ] is  $0.75 \mu\text{m}$ , and the spot-size ( $w_0$ ) is 0.3 mm. The refractive indices of the air, dielectric (AgI) and material (Ag) are  $n_{(0)} = 1$ ,  $n_{(AgI)} = 2.2$ , and  $n_{(Ag)} = 13.5 - j75.3$ , respectively. The value of the refractive index of the material at a wavelength of  $\lambda = 10.6 \mu\text{m}$  is taken from the table performed by Miyagi et al. [3].

#### Toroidal Dielectric waveguides

One of the parameters that we studied was the output power transmission as a function of the radius of curvature. The transmitted fields at  $\zeta = 0^+$  of the initial fields ( $TEM_{00}$  mode in excitation) are formulated by using Fresnel coefficients [Eqs. (2a) to (2d)].

The results of the effect of bending on the output power transmission for the vertical and horizontal polarizations were shown in the case of the optimal dielectric coating [ $d_{(AgI)} = 0.8 \mu\text{m}$ ] by the theoretical ray model [8]. In both polarizations, the results are shown to be the same results by addition of the dielectric layer. Horizontal polarization ( $E_{//}$ ) is defined as parallel to the bending plane (parallel to Y-axis, as shown in Fig. 1, and vertical polarization as perpendicular to it.

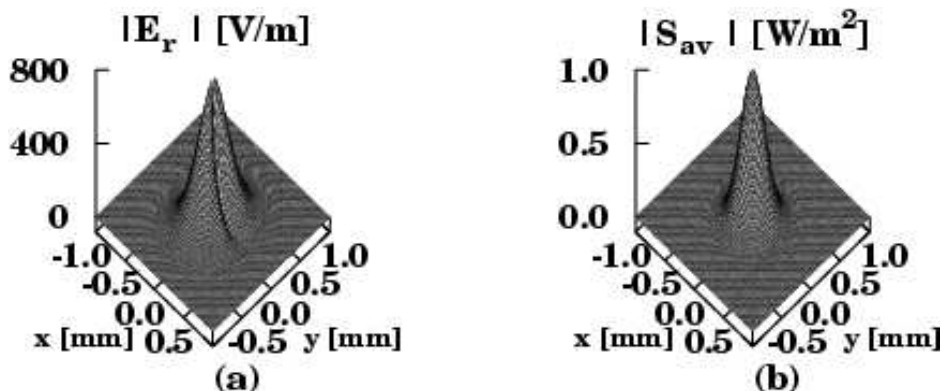


Fig. 2. Solution of the output transverse component of the fields (e.g.,  $|E_r|$  component) and the power density [ $a=1 \text{ mm}$ ,  $d_{(AgI)}=0.75 \text{ mm}$ ,  $\lambda=10.6 \mu\text{m}$ ,  $w_0 = 0.3 \text{ mm}$ ,  $n_{(0)} = 1$ ,  $n_{(AgI)} = 2.2$ ,  $n_{(Ag)} = 13.5 - j 75.3$ , and  $\zeta(R=\infty) = 1 \text{ m}$ ], by letting  $R \rightarrow \infty$ : (a) the output field  $|E_r|$  and (b) the output power density ( $|S_{av}|$ ).

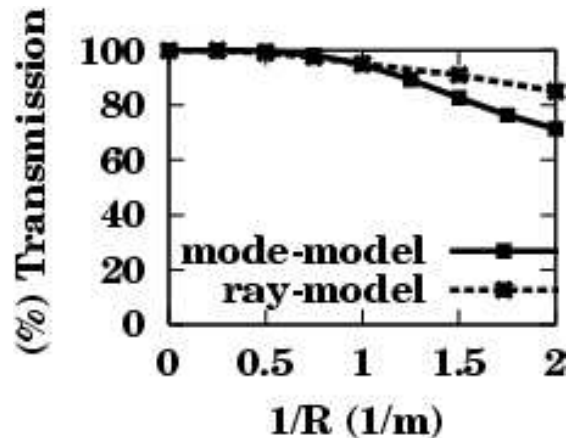


Fig. 3. Theoretical mode model's result and the theoretical ray model's result [8] where the hollow metal waveguide (Ag) covered inside the walls with a AgI film. The power transmission as a function of the radius of curvature for  $\zeta = 1$  m [ $a = 1.5$  mm,  $d_{(AgI)} = 0.8$   $\mu\text{m}$ ,  $w_0 = 0.06$  mm,  $\lambda = 10.6$   $\mu\text{m}$ ,  $n_{(0)} = 1$ ,  $n_{(AgI)} = 2$ , and  $n_{(Ag)} = 10 - j 60$ ].

Fig. 3 shows the results of the theoretical mode model and the theoretical ray model [8] where the length of the curved waveguide ( $\zeta$ ) is 1 m, the diameter ( $2a$ ) of the waveguide is 3 mm, and the spot size ( $w_0$ ) is 0.06 mm. The refractive indices of the air, dielectric, and material are  $n_{(0)} = 1$ ,  $n_{(AgI)} = 2$ , and  $n_{(Ag)} = 10 - j 60$ , respectively. The results of the theoretical mode model and the theoretical ray model [8] give a good approximation, where the waveguide's diameter ( $2a$ ) is much larger than the wavelength ( $2a \gg \lambda$ ).

Fig. 3 shows the dependence of the power transmission as a function of the bending ( $1/R$ ), where  $R$  is the radius of the bending. For small values of  $1/R$  the power transmission is large and decreases with increasing the bending ( $1/R$ ). The metal (Ag) and dielectric (AgI) layers increase the power transmission for both theoretical mode model and theoretical ray model [8].

This example demonstrates the influence of the bending where we take into account all the terms in the calculations (namely, up to the fourth order of  $1/R$ ). This will enable us to understand more precisely the influence of the bending on the output power transmission of hollow waveguides. The results of the output transverse components of the fields, the output power density, and the output power transmission are obtained for a large ( $R \gg r$ ) and a medium ( $R \approx 0.5$  m) radius of curvature.

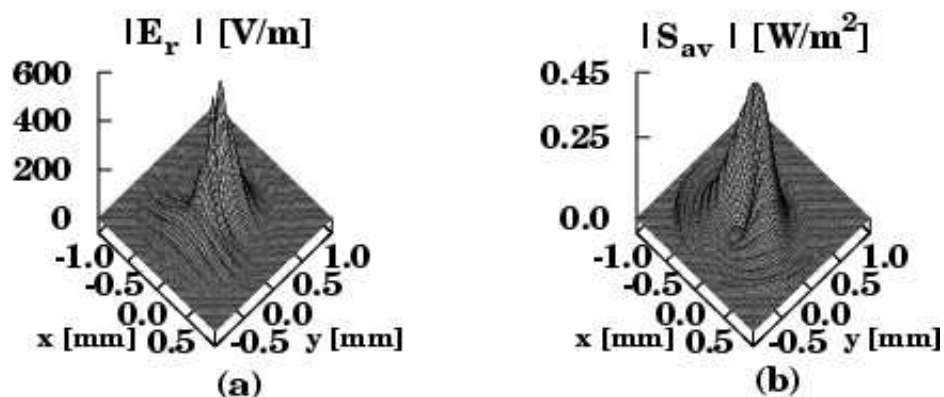


Fig. 4. Solution of the output transverse component of the fields (e.g.,  $|E_r|$  component) and the power density [ $a = 1$  mm,  $d_{(AgI)} = 0.75$   $\mu\text{m}$ ,  $\lambda = 10.6$   $\mu\text{m}$ ,  $w_0 = 0.3$  mm,  $n_{(0)} = 1$ ,  $n_{(AgI)} = 2.2$ ,  $n_{(Ag)} = 13.5 - j 75.3$ ,  $R = 0.7$  m, and  $\phi = \pi$ ]: (a) the output field  $|E_r|$  and (b) the output power density ( $|S_{av}|$ ).

Fig. 4 represents the solution for the output transverse components of the fields (e.g.,  $|E_r|$ ) and the output power density in the case of toroidal dielectric waveguide (Fig. 1), where  $R=0.7$  m and  $\phi = \pi$ . In this example the diameter (2a) of the waveguide is 2 mm, the thickness of the dielectric layer [ $d_{(AgI)}$ ] is  $0.75 \mu\text{m}$ , and the spot size ( $w_0$ ) is 0.3 mm. The values of the refractive indices of the air, dielectric (AgI) and material (Ag) are  $n_{(0)}=1$ ,  $n_{(AgI)} = 2.2$ , and  $n_{(Ag)} = 13.5 - j 75.3$ , respectively. Fig. 4(a) enables us to understand more precisely the influence of the preceding bending ( $R=0.7$  m) on the output transverse components of the fields (e.g.,  $|E_r|$ ). The output power density in Fig. 4(b) shows that in addition to the main propagation mode, several others secondary modes appear. The amplitude is small as the bending radius (R) is small, and the shape is far from a Gaussian. Note that the amplitude of the output power density in Fig. 4(b) is smaller as regard to the output power density in the case of straight waveguide ( $R \rightarrow \infty$ ), as shown in Fig. 2(b). In the calculations all the terms (namely, up to the fourth order of  $1/R$ ) are taken into account.

#### 4. Conclusions

The objective of this work was to develop a theoretical mode model to provide a numerical tool for the calculation of the output transverse fields and power density also for intermediate radius of curvature ( $R \approx 0.5$  m). Therefore we took into account all the terms (namely, up to the fourth order of  $1/R$ ) in the calculations. Note that all the terms were taken into account without neglecting the terms that belong to the bending. This will enable us to understand more precisely the influence of the bending on the output fields, output power density, and output power transmission of hollow waveguides. The results of the solutions of the power transmission were obtained for a large and a medium radius of curvature. The propagation of the electromagnetic wave along the curved waveguide is computed by *input-output* relations [Eqs. (3a), etc.].

In this paper, we supposed that the modes excited at the input of the waveguide by the conventional  $\text{CO}_2$  laser IR radiation ( $\lambda=10.6 \mu\text{m}$ ) are closer to the *TEM* polarization of the laser radiation. The  $\text{TEM}_{00}$  mode is the fundamental and the most important mode. This means that a cross-section of the beam has a Gaussian intensity distribution. The transmitted fields at  $z = 0^+$  of the initial fields (*TEM*<sub>00</sub> mode in excitation) are formulated by using Fresnel coefficients [Eqs. (2a) to (2d)]. The mode model was developed to predict the transmission of energy as a function of the curvature for a given  $\zeta$ . For small values of  $1/R$  the power transmission is large and decreases with increasing the bending ( $1/R$ ). The metal and dielectric layers increase the power transmission for both theoretical mode model and theoretical ray model [8].

The elements of the boundary conditions for  $\text{TEM}_{00}$  mode in excitation are functions of  $1/R^2$ . Miyagi et al. [3] suggested an improved solution in the case of *TE*<sub>01</sub> mode by taking into account the terms correct up to the second order ( $1/R^2$ ), thus their solution provided agreement with the experimental results. We can explain why it is necessary to take into account the terms until the second order ( $1/R^2$ ), at least. The elements of the boundary conditions for *TEM*<sub>00</sub> mode in excitation are functions of the principal terms and the other terms of the second order ( $1/R^2$ ). In the same way, one can derive the elements of the boundary conditions for the *TE*<sub>01</sub> mode to calculate the elements that are dependent on  $1/R^2$ . If the bending's terms of the second order are not taken into account in the case of the *TE*<sub>01</sub> mode or the *TEM*<sub>00</sub> mode in excitation, then the elements of the boundary conditions will give us very little influence of the results. In this case, we obtain good results only for the large values of R ( $R \gg r$ ), such as the models based on the perturbation theory. The remaining orders of the bending ( $1/R^3, 1/R^4$ ) in our calculations are given in the elements of the matrices, and do not appear in the elements of the boundary conditions, in the case of the *TEM*<sub>00</sub> mode in excitation. In this case, the orders of the bending ( $1/R^3, 1/R^4$ ) are neglected as regard to

the orders of the bending ( $1/R$ ,  $1/R^2$ ). Thus, the main point is that we must take into account all the terms until the highest value of the order of the bending, as appear in the elements of the boundary conditions of the initial fields, for arbitrary excitation. All these terms must be taken into account to obtain good results of the output fields, output power density, and output power transmission of hollow waveguides also for an intermediate radius of curvature ( $R \approx 0.5$  m).

The test-case for the straight waveguide is obtained by letting  $R \rightarrow \infty$ . The result of the output power density in this case is compared to the results of previously published experimental data [12] of which the behavior has shown good agreement (a Gaussian shape), as expected, except for the secondary small propagation mode.

This model can take into account the cases of smaller  $R$  only if the step's angle ( $\delta_p$ ) is very small, where the condition is given according to  $\delta_p \geq (2a)/(2\pi R)$ .

The calculation of power density has shown that in addition to the main propagation mode, several other secondary modes appear in the case of the toroidal dielectric waveguide. The amplitude is small as the bending radius ( $R$ ) is small, and the shape is far from a Gaussian.

This mode model may also be a useful tool for solving problems of power transmission of microwaves through flexible curved waveguide for application in medical and industrial fields.

## References

- [1] A. Katzir, SPIE Milestone Series **11**, 3 (1990).
- [2] E. A. J. Marcatili, R. A. Schmeltzer, Bell Syst. Tech. J. **43**, 1783 (1964).
- [3] M. Miyagi, K. Harada, S. Kawakami, IEEE Trans. Microwave Theory Tech. **MTT-32**, 513 (1984).
- [4] N. Croitoru, E. Goldenberg, D. Mendlovic, S. Ruschin, N. Shamir, Proc. Soc. Photo-Opt. Instrum. Eng. **618**, 140 (1986).
- [5] M. E. Marhic, Applied Optics **20**, 3436 (1981).
- [6] M. Miyagi, S. Kawakami, IEEE J. Lightwave Technol **LT-2**, 116 (1984).
- [7] M. E. Marhic, E. Garmire, Appl. Phys. Lett. **38**, 743 (1981).
- [8] N. Croitoru, D. Mendlovic, J. Dror, S. Ruschin, E. Goldenberg, Proc. Soc. Photo-Opt. Instrum. Eng. **713**, 6 (1986).
- [9] N. Croitoru, J. Dror, E. Goldenberg, D. Mendlovic, S. Ruschin, Fiber and integrated Optics **6**, 347 (1987).
- [10] O. Morhaim, D. Mendlovic, I. Gannot, J. Dror, N. Croitoru, Optical Engineering **30**, 1886 (1991).
- [11] D. Mendlovic, E. Goldenberg, S. Ruschin, J. Dror, N. Croitoru, Appl. Opt. **28**, 708 (1989).
- [12] N. Croitoru, A. Inberg, A. Shefer, M. Ben-David, Proc. SPIE/Biomedical Optics **2977**, 30 (1997).